Research Article

SCI

Received: 16 October 2019 Revised: 30 January 2020 Accepted article published: 7 March 2020 Published online in Wiley Online Library: 1 April 2020

(wileyonlinelibrary.com) DOI 10.1002/jsfa.10372

Aptamer-based ellipsometric sensor for ultrasensitive determination of aminoglycoside group antibiotics from dairy products

Mustafa Oguzhan Caglayan*

Abstract

BACKGROUND: Residual antibiotics taken along with food consumed through the food chain are the main cause of the super-bacteria and may damage organs such as liver and kidney. Therefore, monitoring residual antibiotic levels of products in the food chain is both important and a requirement. Maximum residual limits for kanamycin and neomycin are 150 ng mL^{-1} and 500 ng mL^{-1} respectively, which are challenging for most sensor platforms. In this paper, a novel method is presented for the determination of antibiotics residues in animal-derived foods.

RESULTS: Aptamer-based kanamycin and neomycin biosensors based on the spectroscopic ellipsometer and the surface plasmon resonance-enhanced total internal reflection ellipsometer methods as transducing element were developed. Detection limits of both sensor platforms were in the 0.1–1 nmol L^{-1} ranges, and the detection range was between the detection limit and 1000 nmol L^{-1}.

CONCLUSION: Both ellipsometry-based aptasensors can be used as an alternative to the existing enzyme-linked immunosorbent assay-based method in terms of assay time (10 min), detection limit (0.22 ng mL^{-1} for neomycin and 0.048 ng mL^{-1} for kanamycin), and detection range.

Keywords: aminoglycoside antibiotics; biosensors; ultrasensitive analysis; aptamer; surface plasmon resonance; ellipsometry

INTRODUCTION

Antibiotics are extensively used to kill or inhibit microorganisms. However, misuse of antibiotics both causes various side effects in humans and also causes super-bacteria that are tolerant to most antibiotics.[1] An individual may be exposed to certain doses of antibiotics as a result of antibiotics carried by the food chain. For example, trace amounts of kanamycin residues in foodstuffs cause pathogenic bacteria species to develop antibiotic resistance, which could endanger the consumer.[2] Therefore, it is very important to develop sensors to test whether food products contain residual antibiotics within the maximum residue limits (MRLs).[3]

Aminoglycoside antibiotics are used in animal husbandry at very high rates. Kanamycin, an aminoglycoside group of antibiotics, is produced by fermentation from *Streptomyces kanamyceticus*.[4] Kanamycin is used in the treatment of severe infections caused by species such as *Escherichia coli*, *Proteus species*, *Enterobacter aerogenes*, *Klebsiella pneumoniae*, *Serriata marcescens*, *Acinetobacter* spp., and *Mycobacterium tuberculosis*.[5] Kanamycin has a very narrow safety range and has side effects such as hearing loss, toxicity to the kidneys, and allergic reactions to drugs.[6] The EU set the MRL for foods at 100 μg kg^{-1} of meat, 600 μg kg^{-1} of the liver, 2500 μg kg^{-1} of kidney and 150 μg kg^{-1} of milk.[7] Neomycin is another aminoglycoside antibiotic, produced by *Streptomyces fradiae*, that shows excellent activity against Gram-negative bacteria and is also partially active against Gram-positive bacteria.[8] Neomycin is used extensively in the treatment of gastrointestinal infections of bovine animals.[9] Neomycin, like other aminoglycoside antibiotics, is known to be ototoxic and nephrotoxic for humans and animals. The EU has established MRLs for neomycin (500 μg kg^{-1} of meat, 1500 μg kg^{-1} of milk) for consumer protection.[10]

A variety of analytical methods have been developed to verify these limits. Methods for the determination of kanamycin to control drug levels include microbiological methods,[11] fluorescence immunoassay,[12] fluorescence polarization immunoassay, fluorometric assay,[13] and chemiluminescence immunoassay.[14] High-performance liquid chromatography,[15] square-wave cathodic adsorptive stripping voltammetry,[16] immunoanalysis,[17] capillary

* *Correspondence to: MO Caglayan, Bioengineering Department, Bilecik Seyh Edebali University, 11230, Bilecik, Turkey. E-mail: caglayanmoguzhan@gmail.com; oguzhan.caglayan@bilecik.edu.tr*

† *This work has been carried out in Cumhuriyet University Nanotechnology Department, Sivas, Turkey*

Bioengineering Department, Bilecik Seyh Edebali University, Bilecik, Turkey

electrophoresis,[18] surface plasmon resonance (SPR),[19] and microbiological multiple residue system.[20] The most commonly used method for the determination of antibiotics is enzyme-linked immunosorbent assay (ELISA).[21] In addition, chromatographic methods are sensitive and reliable. Owing to its specificity, sensitivity, and low cost, ELISA is frequently used in the determination of antibiotics in food products.[22,23]

Other methods have also shown good analytical performances (Table 1). In a liquid chromatography method, the limit of detection (LOD) and the quantization limit were reported as 1.7 ng mL^{-1} and 5 ng mL^{-1} respectively.[5] In another study using solid-phase extraction and capillary electrophoresis, the LOD was 2 μg mL^{-1}.[26] Yu *et al.*[7] proposed a label-free immunoassay for the determination of kanamycin. In their study, silver hybrid mesoporous iron oxide nanoparticles (NPs) and thionine-mixed graphene sheets were used, in a voltammetric assay with an LOD of 15 pg mL^{-1}.[7] In an amperometric immunoassay, a 5.74 pg mL^{-1} LOD was obtained using a graphene sheet–Nafion/thionine/platinum NP-modified electrode.[31] A 1 nmol L^{-1} LOD has been reported using gold (Au) NPs, in a colorimetric assay.[32] Chen *et al.*[33] developed an immunoassay using magnetic relaxation switching and supermagnetic iron oxide NPs containing a biotin–streptavidin system, and the reported LOD was 0.1 ng mL^{-1}.[33] A very low LOD (6.31 pg mL^{-1}) has been reported in an electrochemical immunoassay where graphene/Prussian blue–chitosan/nanoporous Au composite films were used.[27]

Various methods for the determination of neomycin (and their derivatives) are also available in the literature. Liquid chromatography[34] and ELISA[21] methods have been developed and applied for the determination of neomycin in food products. For example, an LOD of 7.63 nmol L^{-1} and a linear detection region of 9 nmol L^{-1} to 7 μmol L^{-1} have been reported in a study using the molecular suppression and electrochemical sensor pair.[35] The electrochemical behavior of neomycin on the Au electrode modified using a non-specific DNA fragment has been examined and a 0.15 μmol L^{-1} LOD was reported.[36] An amperometric assay developed by immobilization of monoclonal neomycin antibody on a conductive polymer resulted in a linear detection region between 10 and 250 ng mL^{-1} with a 6.76 ng mL^{-1} LOD.[8] Some of the neomycin detection methods are also summarized in Table 1. However, many of these methods summarized herein are not specific and selective, and the results of the analysis are affected and varied when other aminoglycoside antibiotics are present.[26]

Aptamers are good candidates as recognition elements since they can bind to a wide range of target molecules, such as drugs, proteins, or other inorganic molecules, with high affinity and specificity.[37,38] These molecules are obtained by an *in vitro* screening/selection method called systematic evolution of ligands by exponential enrichment.[39,40] There are a limited number of publications on the detection of aminoglycoside group antibiotics by aptamers in the literature. Leung *et al.*[41] suggested the first oligonucleotide-based luminescence assay for the determination of kanamycin in aqueous solutions (LOD 143 nmol L^{-1}). Their result is comparable to the previously reported electrochemical- (2000 nmol L^{-1} LOD),[42] colorimetric- (25 nmol L^{-1} LOD),[43] and Au-nanocomposite-based (9 nmol L^{-1} LOD)[27] analysis methods. In another study,[44] researchers also reported a voltammetric method using anti-tobramycin aptamer for antibiotic analysis, and they obtained a detection limit of 3.44 nmol L^{-1} and a linear range between 6.9 and 300 nmol L^{-1}. In a study using anti-kanamycin aptamer, a detection limit of 25 nmol L^{-1} was reported with an Au-NP-based colorimetric detector.[43] In another voltammetric study, anti-kanamycin aptamer was used on a conductive polymer/Au NP, and a 9.4 nmol L^{-1} LOD with a 50 nmol L^{-1}–9 μmol L^{-1} detection range were reported.[2] Bai *et al.*[45] proposed a cantilever-based aptasensor and determined its performance for kanamycin. They reported a 50 μmol L^{-1} LOD and a linear detection range of 100 μmol L^{-1}–10 mmol L^{-1}. In a study where Faradaic-electrochemical impedance spectroscopy and an RNA aptamer was implemented for the determination of tobramycin, a 1.8 μmol L^{-1} LOD and a linear range between 3 and 72.1 μmol L^{-1} was reported for serum samples.[46] The 2′-*O*-methylated RNA aptamer (5′-GGCCU GGGCG AGAAG UUUAG GCC-3′), which is also used in the study, was used for neomycin-B detection using the SPR sensor. In that study, a 10 nmol L^{-1} LOD was reported.[47]

In this study, techniques involving spectroscopic ellipsometry (SE) and SPR-enhanced (SPRe) total internal reflection ellipsometry (TIRE) were used. The SPR technique is a proven technique for the simultaneous monitoring of many bio-affinity reactions. There are examples in the literature regarding the use of SE and

Table 1. Analytical performances of some of the kanamycin and neomycin determination methods

Method	Linear range/detection range	LOD	Reference
Kanamycin			
Liquid chromatography/liquid chromatography–evaporative light scattering	4–36 μg mL^{-1}	0.2 μg mL^{-1}	24
ELISA	—	0.83 ng mL^{-1}	25
ELISA	—	21 ng mL^{-1}	17
SPR	—	0.48 μg mL^{-1}	19
Capillary electrophoresis	0.4–5 μg mL^{-1}	0.1 μg mL^{-1}	26
Electrochemical immunosensor	0.02–14 ng mL^{-1}	6.31 pg mL^{-1}	27
SE	0.002–0.48 μg mL^{-1}	0.89 ng mL^{-1}	This study
SPRe-TIRE	0.005–0.48 μg mL^{-1}	0.048 ng mL^{-1}	This study
Neomycin			
Amperometry	6 mg L^{-1}–1.22 μg L^{-1}	6 mg L^{-1}	28
ELISA	32–427 μg L^{-1}	32 μg L^{-1}	29
ELISA – direct	10 μg L^{-1}–1 mg L^{-1}	2.73 μg L^{-1}	21
High-performance liquid chromatography	0.2–1 μg g^{-1}	0.1 μg g^{-1}	30
SE	0.003–0.72 μg mL^{-1}	1.55 ng mL^{-1}	This study
SPRe-TIRE	0.007–0.72 μg mL^{-1}	0.22 ng mL^{-1}	This study

SPRe-TIRE in biosensor applications.[48–50] The methods of ellipsometry (and SE) precisely determine the optical properties of ultra-thin films by examining the change in polarization states of light reflected from a surface through a thin film. In addition to this method, TIRE, which is operated under SPR conditions, is a technique in which a simultaneous molecular deposition can be monitored using a flow-cell configuration.[50] In both techniques, the interaction between the target and the diagnostic element can be determined in detail as a result of the ultra-precise determination of surface deposits. A detailed application of these methods for the specific and sensitive determination of aminoglycoside group antibiotics (kanamycin and neomycin in this case) is reported in this paper.

MATERIALS AND METHODS

Chemicals and instrumentation

All chemicals used in this study are Sigma-Aldrich, Merck or Alfa Aesar products; unless specified otherwise, analytical-grade materials were used without further purification. Water used for the preparation of buffers/solutions was ultrapure water (18 MΩ, Human Power; Human Corporation, Seoul, Korea). A plasma cleaning procedure was performed using a Diener model plasma device (at 100 W; Diener Electronic GmbH, Ebhausen, Germany). Surface thickness was measured using an ellipsometer (with spectrophotometric setup, and manual goniometer, Optosense S6000; Optosense, Orlando, FL, USA). The roughness of the sensor chips was determined using an atomic force microscope (XE100; Park Systems Corp, Suwon, Korea).

Repeatability and the presentation of data

Immobilization conditions were determined using at least three replicates. Sensor calibration curves were drawn using three replicates. Selectivity tests and real sample tests were carried out using at least two replicates. Except where stated otherwise, data reported here are the mean of replicates with 1σ.

Aptamer immobilization

The anti-kanamycin aptamer used in this study consists of the main sequence 5′-TGG GGG TTG AGG CTA AGC CGA C-3′ which has been reported by Bai *et al.*[45] The 5′-GGC CUGGG C-GA GAA GUU UAG GCC-3′ RNA aptamer sequence reported by González-Fernández *et al.*[46] was used as the anti-neomycin aptamer. The reported affinity constants are ~80 nmol L^{-1} and ~100 nmol L^{-1} for kanamycin and neomycin respectively in this paper. To immobilize these aptamers to two different platforms, thiol- and amine-functionalized anti-kanamycin/anti-neomycin aptamers were provided (Ella Biotech GmbH, Planegg, Germany). The sequence of aptamers and their terminations used in this study are given in Table 2. The aptamers mentioned are high-affinity aptamers with low disassociation coefficients. A 2′-*O*-methylated form of the same aptamer probe with unprotected RNA aptamer for control was used to prevent the degradation of RNA aptamers by enzymes in samples such as milk. For immobilization and other experiments, all containers to be used during the neomycin experiments were cleaned with ribonuclease (RNase) blocker RNaseZAP®. Cleaning was carried out according to the user instructions.

Before immobilization of the thiolated aptamer sequences, the sensor chip surfaces (glass slides with a 50 nm Au film-coated refractive index of 1.58 at 20° C) were immersed in these solutions in sequence for 2 s: a piranha solution (sulfuric acid and hydrogen peroxide, 7:3 v/v), deionized water, followed by ethyl alcohol. The coating was carried out in the form of 50 nm Au over 3 nm Cr coating using physical vapor deposition apparatus on glass slides that had previously been cleaned and treated with plasma. The sensor chips were then cleaned under air plasma.

The AntiKnm1, AntiKnm2, AntiNeo1, and AntiNeo2 aptamers (0.01–1.0 μmol L^{-1}) in buffer (0.01 mol L^{-1} 4-(2-hydroxyethyl)-1-piperazineethanesulfonic acid (HEPES), 0.15 mol L^{-1} sodium chloridel, 3 mmol L^{-1} ethylenediaminetetraacetic acid, and 0.005% Tween 20) were immobilized on the cleaned surface. The Au sensor chip surface was then blocked using 6-mercapto 1-hexanol (MCH, 1 mmol L^{-1}) prepared in HEPES buffer. Immobilization steps were monitored using SPRe-TIRE measurements. Surface roughness (as root mean square (RMS)) also were determined by examining the surface topography using an atomic force microscope.

AntiKnm3 and AntiKnm4 and AntiNeo3 to AntiNeo5 aptamers were immobilized onto a surface-modified silicon (Si) wafer. Si wafer pieces, cut into approximately 1 × 1 cm^2, were cleaned by plasma treatment for 30 min after wet cleaning with nitric acid, hydrogen peroxide, ethyl alcohol, water, and acetone, subsequently. Dimensions of flakes were taken approximately equal due to their importance in terms of mass transfer and binding kinetics, since immobilization would be performed based on the self-assembling of silanol groups by immersion. After cleaning, wafer pieces were taken into contact with mercaptopropyl trimethoxysilane (MPTES) solutions prepared in absolute ethyl alcohol to obtain an SH-terminated monolayer on the Si surface. Surface immobilization was monitored by thickness measurement by SE. After that, a layer having —COOH functionality was

Table 2. Anti-kanamycin and anti-neomycin aptamers used in the study

Probe name	Sequence	Sensor chip surface	Method
AntiKnm1	5′-(SH)-$(CH_2)_6$-TGG GGG TTG AGG CTA AGC CGA C-3′	Au-coated glass	SPRe-TIRE
AntiKnm2	5′-(SH)-$(CH_2)_6$-$(A)_{10}$-TGGGGGTTGAGGCTA AGCCGAC-3′	Au-coated glass	SPRe-TIRE
AntiKnm3	5′-$(NH)_2$-$(CH_2)_6$-TGGGGGTTGAGGCTA AGCCGAC-3′	Si wafer	SE
AntiKnm4	5′-$(NH)_2$-$(CH_2)_6$-$(A)_{10}$-TGGGGGTTGAGGCTA AGCCGAC-3′	Si wafer	SE
AntiNeo1	5′-(SH)-$(CH_2)_6$- GGC CUGGG CGA GAA GUU UAG GCC-3′	Au-coated glass	SPRe-TIRE
AntiNeo2	5′-(SH)-$(CH_2)_6$-$(A)_{10}$-GGC CUGGG CGA GAA GUU UAG GCC-3′	Au-coated glass	SPRe-TIRE
AntiNeo3	5′-$(NH)_2$-$(CH_2)_6$-GGC CUGGG CGA GAA GUU UAG GCC-3′	Si wafer	SE
AntiNeo4	5′-$(NH)_2$-$(CH_2)_6$-$(A)_{10}$-GGC CUGGG CGA GAA GUU UAG GCC-3′	Si wafer	SE
AntiNeo5	5′-$(NH)_2$-$(CH_2)_6$-GGC CUGGG CGA GAA GUU UAG GCC-3′ (2′-fully methylated)	Si wafer	SE

formed on the surface using mercaptoundecanoic acid (MUA). After this process, to be carried out by the route of disulfide interaction, amino-group-terminated aptamers were finally bound to the —COOH-terminated surface by 1-ethyl-3-(3-dimethyl aminopropyl)carbodiimide (EDAC) reaction. In this step, where the concentration and immersion times were optimized, the thickness of the organic layer deposited on the Si surface was also monitored using an ellipsometer.

Kanamycin and neomycin detection by SE and SPRe-TIRE

Si surfaces (sensor chips) on which AntiKnm3, AntiKnm4, or AntiNeo3–AntiNeo5 have been immobilized under the specified conditions were immersed in kanamycin or neomycin in buffer solution (0–1000 nmol L^{-1}). After immersion, the sensor surfaces washed with buffer solution were analyzed by spectroscopic ellipsometer. Because the Si flakes were opaque, the simultaneous measurement could not be performed at this step of the study. After delta (Δ) and psi (Ψ) measurements performed in the whole spectrum (200–1700 nm wavelength), the amount of analyte captured by the aptasensor immobilized on the sensor chip was evaluated in terms of Δ changes. The Δ angle (i.e. the phase shift between polarization states) shifted to lower degrees since the surface build-up changes the thickness and refractive index (real and imaginary) of the surface film. The sensor calibration graph (Δ change *vs* target concentration) was drawn and the LOD of the sensor was determined. Tobramycin was used to determine the specificity. After the determination of specificity and noise (NR) values, the theoretical determination limit (3σ) of the sensor was also reported. Additionally, surface thicknesses after capturing the target molecules were determined by ellipsometric measurements. Surface roughness was also examined using topography images obtained from the atomic force microscope in contact mode using CM-silicon probes (Park Systems Corp.). The roughness analyses were performed on ten different points in ten scanning areas on at least four samples. The schematic representation of ellipsometric methods and typical sensor responses are shown in Fig. 1.

Kanamycin or neomycin solutions prepared in buffer solution, in this part, were brought into contact with Au surfaces prepared under specified conditions. A total internal reflection device and a flow system (i.e. similar to SPR) were used as a requirement of the SPRe-TIRE configuration. For this purpose, AntiKnm1 and AntiKnm2 and AntiNeo1 and AntiNeo2 sensor chips immobilized on the Au-coated BK7 glass surface were washed with buffer solution (HEPES) in a flow-cell comprising a BK7 glass prism coupled with a refractive-index-matching oil (refractive index 1.58). Then, kanamycin/neomycin solutions in the buffer (0–1000 nmol L^{-1}) were injected in the flow-cell of the spectroscopic ellipsometer. First, delta (Δ) and psi (Ψ) measurements were performed in the whole spectrum (i.e. between 200 and 1700 nm). Then, analysis was performed in the region close to the wavelength (65° and 780 nm) where the SPR phenomenon has been determined (where Δ has infinite slope). Antibiotics amount captured by the aptasensor immobilized on the sensor chip was evaluated in terms of Δ changes. Sensor performance and specificity were determined using methods similar to those described in the previous section.

Table 3. Ellipsometric thickness and RMS roughness for 0.1 μmol L^{-1} AntiKnm2 probe immobilization

Time (s)	Thickness (nm)	RMS roughness (nm)
60	0.74 ± 0.11	1.20 ± 0.08
120	1.25 ± 0.14	1.35 ± 0.12
240	1.84 ± 0.13	2.21 ± 0.18
300	2.03 ± 0.11	2.81 ± 0.23
7200	2.08 ± 0.10	3.02 ± 0.52

RESULTS AND DISCUSSION

Immobilization conditions on Au or Si surface

The Au-coated glass slide was used to get plasmon resonance to operate the biosensor system under SPRe-TIRE conditions. The immobilization time of the aptamers on this surface and the aptamer concentration parameters were optimized. The real-time signal obtained after injection of the probe in the buffer solution has reached approximately an equilibrium within 5 min. Sensor surfaces were washed with a buffer solution after injection performed for various durations. The surface build-up thickness was then measured using a spectroscopic ellipsometer (Table 3) to

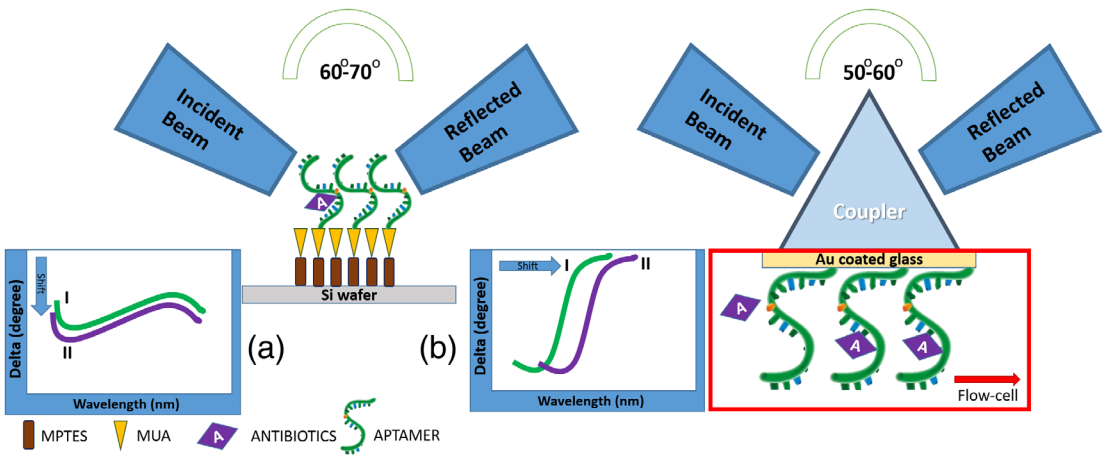

Figure 1. Schematic representation of ellipsometric methods and their typical sensor responses for (a) SE and (b) SPRe-TIRE. Schematic graphs for sensor response *versus* wavelength represent usual sensor signals before (I) and after (II) target capturing. A 'shift' arrow represents the corresponding delta shift (i.e. sensor signal in our case) upon target capturing.

Table 4. Probe immobilization optimums for SPRe-TIRE probes

Aptamer	Time (s)	Concentration (μM)	Detector signal change Δ at optimums (deg)
AntiKnm1	300	1.00	5.20 ± 0.05
AntiKnm2	300	1.00	5.51 ± 0.05
AntiNeo1	300	1.00	5.27 ± 0.06
AntiNeo2	300	1.00	5.73 ± 0.05

optimize immobilization time. According to the results, 5 min was appropriate, where significant thickness change cannot be observed further.

The surface thickness obtained from the ellipsometric modeling using library parameters for BK7/Cr/Au/1.46 organic/air materials, was become steady around 300 s. Furthermore, it was observed that the roughness obtained from topography measurements increased, whereas the uniformity (as standard deviation) decreased with the immobilization. The roughness of the bare Au surface is close to that obtained for 60 s (0.81 ± 0.09), as shown in Table 3. This shows that the probe distribution becomes non-uniform for longer contact times. Consequently, 5 min immobilization using a 1.00 μmol L^{-1} aptamer probe and purging with a buffer for 2 min was deemed as optimum immobilization conditions for aptamer probes. Optimized immobilization conditions for other Au-surface-related probes and observed signals received under these conditions are given in Table 4.

The AntiKnm2 and the AntiNeo2 are larger than other aptamers with an additional ten A bases; therefore, a higher signal was expected. However, values shown in Table 4 were very close to each other, which may be the result of the diffusion limitations. After this step, blocking was performed using 1 mmol L^{-1} MCH in the buffer, to minimize non-specific interactions and to reduce the interaction of the oligonucleotide with the Au surface. The physically unbound MCH layer was then removed by washing with buffer solution after 5 min of immersion.

For the SE-based assay, on the contrary, the Si surface was used as a substrate. First, concentration and immersion time optimization were performed for the self-assembling phase of MPTES. An Si substrate, silicon dioxide (SiO_2) layer, and organic layer as the Cauchy model and air as a medium were used as model parameters for ellipsometric modeling, which are available in the equipment's library. The layer thickness on the Si surface using 1 μmol L^{-1} MPTES after 1–8 h dipping was then monitored. During the first 2 h, a near-monolayer formation (as thickness) was observed. However, the increase in thickness for longer periods could be a result of the accumulation of MPTES on the surface, due to water vapor ingress from the air. Consequently, optimum MPTES immobilization time and concentration were determined to be 2 h (in the dark, at room temperature) and 1.0 μmol L^{-1} respectively. After the determination of MPTES immobilization conditions, MUA was used to get —COOH functionalized surface. The disulfide reaction was carried out for 2–24 h, using 1.0 μmol L^{-1} MUA at room temperature, in the vacuumed and nitrogen-swept closed vessels at dark. Ellipsometric thickness (by assuming Si/SiO_2/organic layer (defined by Cauchy Model)/air) and RMS roughness were used for optimization purposes, as described before. It was observed that immersion times ≥8 h were appropriate for immobilizing the MUA on MPTES, as an overlayer. The optimum MUA concentration was 5 μmol L^{-1}, where the thickness and roughness were almost steady.

For the immobilization of AntiKnm3, AntiKnm4 and AntiNeo3, and AntiNeo4 and AntiNeo5 aptamers onto the —COOH terminated surface via the EDAC route, probe solutions in the buffer (0.1–2 μmol L^{-1}) were immobilized for 2 h (Fig. 2). Additionally, ellipsometric thickness measured after immobilization of 1.5 μmol L^{-1} probe on the —COOH-functionalized surface for 10–240 min reached a steady level (2.71 ± 0.13 nm) at 120 min, which also was selected as optimum.

Sensor performance of SE and SPRe-TIRE

The ellipsometric angle Δ for each Si sensor chip gave a linear $\Delta-\lambda$ relationship between 600–700 nm with a regression coefficient of 0.94, since the material deposited on the surface as an organic layer upon target–aptamer interaction. This linear response zone shifted to the lower Δ degrees upon the interaction between the kanamycin/neomycin and the aptamer probe. The calibration curves for all SE assays used in this study were obtained using this correlation. The analytical performance of AntiKnm1, AntiKnm2, AntiNeo1, and AntiNeo2 aptamers immobilized on the Au surface as kanamycin and neomycin sensors was also tested. The ellipsometric angle Δ was continuously measured using a flow-cell at a 5 μL min^{-1} flow rate and at room temperature. Δ values shifted to the lower degrees upon the interaction between the antibiotics and the aptamer probe. The calibration curves for all SPRe-TIRE assay probes were obtained using this time-dependent correlation. All sensor responses were linear at low target concentrations, whereas overall responses were exponential due to the nature of the aptamer–target interaction.

Calibration curve parameters

Calibration curves for all assays were modeled to easily compare assay performances *via* model parameters. The Langmuir model (Eqn (1)) and the Belehradek model (Eqn (2)) parameters are

$$\Delta = \frac{a \times b(\text{Antibiotics Concentration})^{1-c}}{1 + b(\text{Antibiotics Concentration})^{1-c}} \quad (1)$$

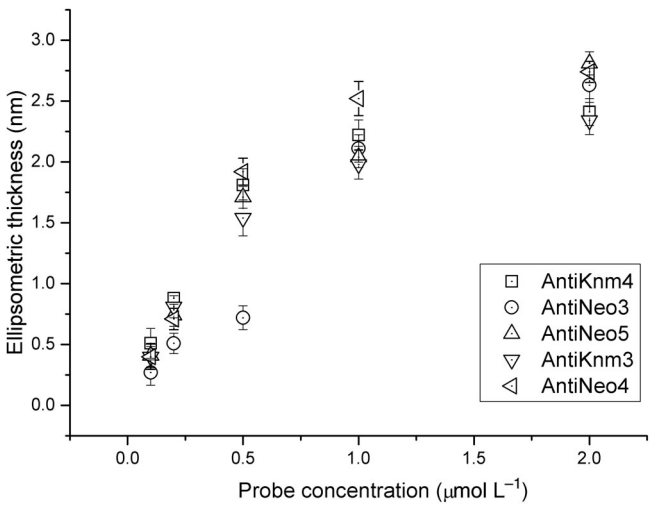

Figure 2. The ellipsometric thickness of sensor surfaces after immobilization of AntiKnm3, AntiKnm4, AntiNeo3, AntiNeo4, and AntiNeo5 at different concentrations (room temperature, 2 h).

Table 5. SE and SPRe-TIRE calibration parameters and LODs

Aptamer	Model parameters	Regression coefficient R^2	LOD (3σ, nmol L^{-1})
SE			
AntiKnm3	$a = 6.5421$	0.91	1.84
	$b = 0.1282$		
	$c = 0.2941$		
AntiKnm4	$a = 5.9643$	0.86	4.00
	$b = 0.0967$		
	$c = 0.2157$		
AntiNeo3	$a = 4.7173$	0.88	6.88
	$b = 0.3638$		
	$c = 0.5210$		
AntiNeo4	$a = 4.2123$	0.86	6.68
	$b = 0.7441$		
	$c = 0.4319$		
AntiNeo5	$a = 5.1244$	0.81	2.52
	$b = 0.7548$		
	$c = 0.3145$		
SPRe-TIRE			
AntiKnm1	$a = 9.5839$	0.98	0.10
	$b = 0.0103$		
	$c = 0.2720$		
AntiKnm2	$a = 10.5379$	0.94	2.91
	$b = 0.0571$		
	$c = 0.25816$		
AntiNeo1	$a = 8.1265$	0.98	0.36
	$b = 0.0219$		
	$c = 0.11529$		
AntiNeo2	$a = 7.05824$	0.95	0.97
	$b = 0.0065$		
	$c = 0.1448$		

$$\Delta = a(\text{Antibiotics Concentration} + b)^c \quad (2)$$

Both models are suitable for single-site interaction, which describes aptamer and target interaction. All probe–antibiotics interactions in this study fit the Belehradek model with a regression coefficient of 90%, approximately, whereas Langmuir models were below 80%. Consequently, model 2 (i.e. Belehradek) was chosen, and its parameters (*a*, *b*, and *c*) are listed in Table 5 along with the corresponding regression coefficients. The LOD for each assay was calculated using the standard deviation (as 3σ) of the measured lowest concentration. The LODs for all aptamer assays are also reported in Table 5.

Sensor responses obtained by SE were very similar for the range investigated, including ten adenine-base-containing probes. The lowest LODs were 1.84 nmol L^{-1} (0.89 ng mL^{-1}) and 2.52 nmol L^{-1} (1.55 ng mL^{-1}) for kanamycin and neomycin respectively. Both LODs are below the established residue limits for kanamycin and neomycin[7,10] and within comparable limits to the ELISA-based method reported for kanamycin and neomycin.[21,25]

To check the interference, 100 nmol L^{-1} tobramycin was added to the buffer solution containing 100 nmol L^{-1} kanamycin/neomycin. In addition, the sensor response for only 100 nmol L^{-1} tobramycin-containing buffer solution was measured to determine specificity. The specificity and selectivity results are reported in Fig. 3. The specificity of aptamers to their target was successfully demonstrated since the tobramycin resulted in a signal increase of less than 10% of the actual response.

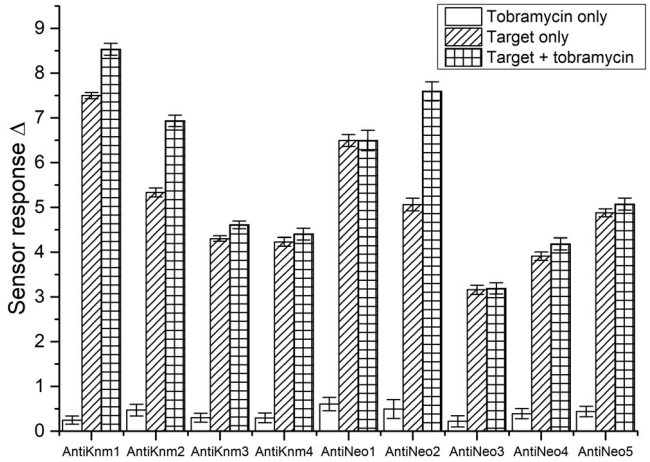

Figure 3. Selectivity of SE and SPRe-TIRE sensors. Sensor responses for tobramycin, target (kanamycin/neomycin) and target + tobramycin.

Finally, all assays were checked for the real sample applicability using kanamycin and neomycin determination in pasteurized, commercial milk samples prepared according to the literature.[51] A mid-range amount (100 nmol L^{-1}) and a lower-range amount (10 nmol L^{-1}) kanamycin and neomycin solutions were spiked in milk samples, and the recovered amounts are reported in Table 6. The sensor was successful in detecting kanamycin and neomycin added to the milk. There was no significant difference in the milk sample between the methylated AntiNeo5 sensor and the unmethylated precursor AntiNeo4 sensor because of the RNase blocker.

Table 6. – Sensor performance for real milk samples

Aptamer	Spiked amount (nmol L^{-1})	Determined (nmol L^{-1})	Recovery (%)
AntiKnm1	100	99.85	99.9
	10	10.24	102.4
AntiKnm2	100	99.90	99.9
	10	9.94	99.4
AntiKnm3	100	100.45	100.5
	10	9.97	99.7
AntiKnm4	100	98.62	98.6
	10	9.68	96.8
AntiNeo1	100	98.82	98.8
	10	10.63	106.3
AntiNeo2	100	101.41	101.4
	10	9.84	98.4
AntiNeo3	100	101.72	101.7
	10	10.44	104.4
AntiNeo4	100	99.94	99.9
	10	9.81	98.1
AntiNeo5	100	101.04	101.0
	10	10.32	103.2

CONCLUSIONS

In this study, two different types of aptasensors were developed and compared using SE and SPRe-TIRE for kanamycin and neomycin. The lowest and highest LODs for kanamycin were 100 pmol L^{-1} and 4.00 nmol L^{-1} respectively. The LOD for neomycin was 360 pmol L^{-1} and the highest was 6.88 nmol L^{-1}. Since SPRe-TIRE works in the SPR region where Δ changes rapidly under analysis conditions, detection limits were lower. Moreover, the calibration data fit better in terms of regression coefficients. The sensor performances obtained are high enough for the MRL for kanamycin and neomycin[7,10] and within comparable limits to the ELISA-based method reported for kanamycin and neomycin (0.83 ng mL^{-1} and 2.73 ng mL^{-1} respectively).[21,25]

Although the selectivity of aptamers was known, the antibiotics added to the milk sample prepared with tobramycin at the lowest and mid-range concentrations used in the study were accurately measured. The highest recovery error in milk samples was 6.3% (0.386 ng mL^{-1}) at 10 nmol L^{-1} for AntiNeo1 (positive error). The highest negative error was found to be 3.4% (0.164 ng mL^{-1}) at 10 nmol L^{-1} concentration for AntiKnm4.

Consequently, SE and SPRe-TIRE-based aptasensors can be used as an alternative to the existing ELISA-based method in terms of assay time (10 min), detection limit (0.22 ng mL^{-1} for neomycin and 0.048 ng mL^{-1} for kanamycin), and detection range (MRL is 0.5 μg mL^{-1}).

ACKNOWLEDGEMENTS

This work was supported by the Scientific and Technological Research Council of Turkey (TÜBİTAK), grant no: 214 M608.

REFERENCES

1 Goldman E, Antibiotic abuse in animal agriculture: exacerbating drug resistance in human pathogens. *Hum Ecol Risk Assess Int J* **10**: 121–134 (2004).
2 Zhu Y, Chandra P, Song KM, Ban C and Shim YB, Label-free detection of kanamycin based on the aptamer-functionalized conducting polymer/gold nanocomposite. *Biosens Bioelectron* **36**:29–34 (2012).
3 Kim DM, Rahman MA, Do MH, Ban C and Shim YB, An amperometric chloramphenicol immunosensor based on cadmium sulfide nanoparticles modified-dendrimer bonded conducting polymer. *Biosens Bioelectron* **25**:1781–1788 (2010).
4 Pindell MH, The pharmacology of kanamycin – a review and new developments. *Ann N Y Acad Sci* **132**:805–810 (1966).
5 Manyanga V, Dhulipalla RL, Hoogmartens J and Adams E, Improved liquid chromatographic method with pulsed electrochemical detection for the analysis of kanamycin. *J Chromatogr A* **1217**: 3748–3753 (2010).
6 Oertel R, Neumeister V and Kirch W, Hydrophilic interaction chromatography combined with tandem-mass spectrometry to determine six aminoglycosides in serum. *J Chromatogr A* **1058**:197–201 (2004).
7 Yu S, Wei Q, Du B, Wu D, Li H, Yan L *et al.*, Label-free immunosensor for the detection of kanamycin using Ag@Fe_3O_4 nanoparticles and thionine mixed graphene sheet. *Biosens Bioelectron* **48**:224–229 (2013).
8 Zhu Y, Son JI and Shim YB, Amplification strategy based on gold nanoparticle-decorated carbon nanotubes for neomycin immunosensors. *Biosens Bioelectron* **26**:1002–1008 (2010).
9 MacDonald RH and Beck M, Neomycin: a review with particular reference to dermatological usage. *Clin Exp Dermatol* **8**:249–258 (1983).
10 Jin Y, Jang JW, Han CH and Lee MH, Development of immunoassays for the detection of kanamycin in veterinary fields. *J Vet Sci* **7**:111–117 (2006).
11 Arret B, Johnson DP and Kirshbaum A, Outline of details for microbiological assays of antibiotics: second revision. *J Pharm Sci* **60**: 1689–1694 (1971).
12 DeCastro AF, Place JD, Lam CT and Patel C, Determination of kanamycin concentration in serum by substrate-labeled fluorescent immunoassay. *Antimicrob Agents Chemother* **29**:961–964 (1986).
13 El-Shabrawy Y, Fluorimetric determination of aminoglycoside antibiotics in pharmaceutical preparations and biological fluids. *Spectrosc Lett* **35**:99–109 (2002).
14 Alwarthan AA, Al-Tamrah SA and Akel AA, Flow-injection determination of kanamycin by inhibition of the lucigenin–H_2O_2–Co^{2+} system. *Anal Chim Acta* **292**:201–208 (1994).
15 Zhou YX, Yang WJ, Zhang LY and Wang ZY, Determination of kanamycin A in animal feeds by solid phase extraction and high performance liquid chromatography with pre-column derivatization and fluorescence detection. *J Liq Chromatogr Relat Technol* **30**: 1603–1615 (2007).
16 Yan J-L, Determinationation of kanamycin by square-wave cathodic adsorptive stripping voltammetry. *Russ J Electrochem* **44**: 1334–1338 (2008).
17 Loomans EE, Van Wiltenburg J, Koets M and Van Amerongen A, Neamin as an immunogen for the development of a generic ELISA detecting gentamicin, kanamycin, and neomycin in milk. *J Agric Food Chem* **51**:587–593 (2003).
18 Kaale E, Van Schepdael A, Roets E and Hoogmartens J, Determination of kanamycin by electrophoretically mediated microanalysis with in-capillary derivatization and UV detection. *Electrophoresis* **24**: 1119–1125 (2003).
19 Frasconi M, Tel-Vered R, Riskin M and Willner I, Surface plasmon resonance analysis of antibiotics using imprinted boronic acid-functionalized au nanoparticle composites. *Anal Chem* **82**: 2512–2519 (2010).
20 Althaus R, Berruga MI, Montero A, Roca M and Molina MP, Evaluation of a microbiological multi-residue system on the detection of antibacterial substances in ewe milk. *Anal Chim Acta* **632**:156–162 (2009).
21 Jin Y, Jang JW, Lee MH and Han CH, Development of ELISA and immunochromatographic assay for the detection of neomycin. *Clin Chim Acta* **364**:260–266 (2006).
22 Chen Y, Li X, He L, Tang S and Xiao X, Immunoassays for the rapid detection of gentamicin and micronomicin in swine muscle. *J AOAC Int* **93**:335–342 (2010).
23 Szekeres PG, Leong K, Day TA, Kingston AE and Karran EH, Development of homogeneous 384-well high-throughput screening assays for Abeta1-40 and Abeta1-42 using AlphaScreen technology. *J Biomol Screen* **13**:101–111 (2008).
24 Megoulas NC and Koupparis MA, Direct determination of kanamycin in raw materials, veterinary formulation and culture media using a novel liquid chromatography–evaporative light scattering method. *Anal Chim Acta* **547**:64–72 (2005).
25 Chen Y, Wang Z, Wang Z, Tang S, Zhu Y and Xiao X, Rapid enzyme-linked immunosorbent assay and colloidal gold immunoassay for kanamycin and tobramycin in swine tissues. *J Agric Food Chem* **56**: 2944–2952 (2008).
26 Long YH, Hernandez M, Kaale E, Van Schepdael A, Roets E, Borrull F *et al.*, Determination of kanamycin in serum by solid-phase extraction, pre-capillary derivatization and capillary electrophoresis. *J Chromatogr B Anal Technol Biomed Life Sci* **784**:255–264 (2003).
27 Zhao BY, Wei Q, Xu C, Li H, Wu D, Cai Y *et al.*, Label-free electrochemical immunosensor for sensitive detection of kanamycin. *Sens Actuators B* **155**:618–625 (2011).
28 Leech D, Wang J and Smyth MR, Electrocatalytic detection of streptomycin and related antibiotics at ruthenium dioxide modified graphite–epoxy composite electrodes. *Analyst* **115**:1447–1450 (1990).
29 Knecht BG, Strasser A, Dietrich R, Martlbauer E, Niessner R and Weller MG, Automated microarray system for the simultaneous detection of antibiotics in milk. *Anal Chem* **76**:646–654 (2004).
30 Posyniak A, Zmudzki J and Niedzielska J, Sample preparation for residue determination of gentamicin and neomycin by liquid chromatography. *J Chromatogr A* **914**:59–66 (2001).
31 Wei Q, Zhao Y, Du B, Wu D, Li H and Yang M, Ultrasensitive detection of kanamycin in animal derived foods by label-free electrochemical immunosensor. *Food Chem* **134**:1601–1606 (2012).
32 Zhang X, Zhang Y, Zhao H, He Y, Li X and Yuan Z, Highly sensitive and selective colorimetric sensing of antibiotics in milk. *Anal Chim Acta* **778**:63–69 (2013).
33 Chen YP, Zou M, Qi C, Xie MX, Wang DN, Wang YF *et al.*, Immunosensor based on magnetic relaxation switch and biotin–streptavidin

system for the detection of kanamycin in milk. *Biosens Bioelectron* **39**:112–117 (2013).
34 Zawilla NH, Diana J, Hoogmartens J and Adams E, Analysis of neomycin using an improved liquid chromatographic method combined with pulsed electrochemical detection. *J Chromatogr B Anal Technol Biomed Life Sci* **833**:191–198 (2006).
35 Lian W, Liu S, Yu J, Li J, Cui M, Xu W *et al*., Electrochemical sensor using neomycin-imprinted film as recognition element based on chitosan–silver nanoparticles/graphene–multiwalled carbon nanotubes composites modified electrode. *Biosens Bioelectron* **44**:70–76 (2013).
36 Li X, Chen Y and Huang X, Electrochemical behavior of neomycin at DNA-modified gold electrodes. *J Inorg Biochem* **101**:918–924 (2007).
37 You KM, Lee SH, Im A and Lee SB, Aptamers as functional nucleic acids: *in vitro* selection and biotechnological applications. *Biotechnol Bioproc Eng* **8**:64–75 (2003).
38 Luzi E, Minunni M, Tombelli S and Mascini M, New trends in affinity sensing: aptamers for ligand binding. *TrAC Trends Anal Chem* **22**: 810–818 (2003).
39 Tuerk C and Gold L, Systematic evolution of ligands by exponential enrichment: RNA ligands to bacteriophage T4 DNA polymerase. *Science* **249**:505–510 (1990).
40 Ellington AD and Szostak JW, *In vitro* selection of RNA molecules that bind specific ligands. *Nature* **346**:818–822 (1990).
41 Leung K-H, He H-Z, Chan DS-H, Fu W-C, Leung C-H and Ma D-L, An oligonucleotide-based switch-on luminescent probe for the detection of kanamycin in aqueous solution. *Sens Actuators B Chem* **177**: 487–492 (2013).
42 Rowe AA, Miller EA and Plaxco KW, Reagentless measurement of aminoglycoside antibiotics in blood serum via an electrochemical, ribonucleic acid aptamer-based biosensor. *Anal Chem* **82**:7090–7095 (2010).
43 Song KM, Cho M, Jo H, Min K, Jeon SH, Kim T *et al*., Gold nanoparticle-based colorimetric detection of kanamycin using a DNA aptamer. *Anal Biochem* **415**:175–181 (2011).
44 Sun N, Mo WM, Shen ZL and Hu BX, Adsorptive stripping voltammetric technique for the rapid determination of tobramycin on the hanging mercury electrode. *J Pharm Biomed Anal* **38**:256–262 (2005).
45 Bai X, Hou H, Zhang B and Tang J, Label-free detection of kanamycin using aptamer-based cantilever array sensor. *Biosens Bioelectron* **56**:112–116 (2014).
46 González-Fernández E, de-los-Santos-Álvarez N, Lobo-Castañón MJ, Miranda-Ordieres AJ and Tuñón-Blanco P, Impedimetric aptasensor for tobramycin detection in human serum. *Biosens Bioelectron* **26**: 2354–2360 (2011).
47 De-los-Santos-Álvarez N, Lobo-Castañón MJ, Miranda-Ordieres AJ and Tuñón-Blanco P, SPR sensing of small molecules with modified RNA aptamers: detection of neomycin B. *Biosens Bioelectron* **24**: 2547–2553 (2009).
48 Keske A, Atar A, Üstündağ İ and Çağlayan MO, Detection of influenza A by surface plasmon resonance enhanced total internal reflection ellipsometry. *J Comput Theor Nanosci* **11**:981–986 (2014).
49 Üstündağ Z, Çağlayan MO, Güzel R, Pişkin E and Solak AO, A novel surface plasmon resonance enhanced total internal reflection ellipsometric application: electrochemically grafted isophthalic acid nanofilm on gold surface. *Analyst* **136**:1464–1471 (2011).
50 Çağlayan MO, Sayar F, Demirel G, Garipcan B, Otman B, Celen B *et al*., Stepwise formation approach to improve ellipsometric biosensor response. *Nanomedicine* **5**:152–161 (2009).
51 Song K, Jeong E, Jeon W, Cho M and Ban C, Aptasensor for ampicillin using gold nanoparticle based dual fluorescence–colorimetric methods. *Anal Bioanal Chem* **402**:2153–2161 (2012).

